THE UNIVERSITY OF MICHIGAN

COLLEGE OF ENGINEERING
Department of Aerospace Engineering
High Altitude Engineering Laboratory

Scientific Report

FALLING SPHERE MEASUREMENTS, 30 TO 120 KM

L. M. Jones and J. W. Peterson

(At a Symposium of the American Meteorological Society)
(Miami Beach, Florida, June 2, 1967)

ORA Project 05627

under contract with:

NATIONAL AERONAUTICS AND SPACE ADMINISTRATION
CONTRACT NO. NASr-54(05)
WASHINGTON, D. C.

administered through:

OFFICE OF RESEARCH ADMINISTRATION ANN ARBOR

June 1967

TABLE OF CONTENTS

ABSTRACT

Various versions of the falling sphere experiment have been used since 1952. Spheres equipped with sensitive accelerometers and passive, radar tracked, inflated spheres are discussed. Soundings with the latter system are more prevelant and are discussed in some detail. With the best radars, density is measured to 120 km and winds to 70 km. Problems have to do with the effects of vertical wind, anomalous aerodynamic flow and loss of inflation gas. Flight comparisons with grenades, bead thermistors and mass spectrometers are discussed. Results from falling spheres include profiles for model atmospheres, an explosive warming, a tropical survey in all seasons, a southern hemisphere circulation study, a mesopause thermal fine structure study and a study of the vertical scale of stratospheric and mesospheric winds.

Falling Sphere Measurements, 30 to 120 Km

L. M. Jones and J. W. Peterson
Department of Aerospace Engineering
University of Michigan

Introduction

Falling spheres, carried aloft in rockets, have been used frequently since 1952 to measure density, temperature and winds in the upper atmosphere. The fundamental equation of the experiment is the familiar one of aerodynamic drag

$$F_D = m\, a_D = \tfrac{1}{2}\rho v^2 C_D A \qquad (1)$$

where

F_D = drag force

m = sphere mass

a_D = drag acceleration

ρ = ambient density

v = sphere velocity

C_D = coefficient of drag

A = sphere cross sectional area

Values for C_D as a function of Mach number and Reynolds number are fairly well known from ground measurements carried out in wind tunnels and ballistic tunnels. Having measured density as a function of altitude the equations of state and of hydrostatic pressure are combined to permit the calculation of temperature.

$$T_z = \frac{1}{\rho_z}\left[\frac{M}{R}\int_{z_o}^{z} -\rho_z g\, dz + \rho_o T_o\right] \qquad (2)$$

where

T_z = ambient temperature

z = altitude

z_o = starting altitude

M = gram molecular weight, known from other measurements

R = universal gas constant

g = acceleration of gravity

ρ_o = ambient density at z_o

T_o = ambient temperature at z_o

Typically the integration of density proceeds downward from the starting altitude z_o which is the altitude of the highest valid density data. The arbitrary choice of T_o at this point may introduce an error in the calculated temperature which, however, decreases and becomes negligible by comparison with other errors at a point about 15 km below the starting altitude.

Horizontal wind velocities can be determined from ground-tracking sphere motions. The winds can be computed from the equations of motion or, more simply but less accurately, be taken as equal to the projections of the sphere velocities. Vertical winds are neglected. Some work has been done on the effects of vertical winds and on the small effect of neglecting them. Also it has been shown that vertical winds might be measured by observing simultaneously two spheres of different mass-to-area ratios. The method, however, has not been fully developed.

Several types of sphere experiment systems have been developed and used. Inflatable spheres, with diameters ranging between 0.66 and 2.75 meters,

have large area-to-mass ratios and may be tracked from the ground either by radar or rf interferometers such as DOVAP. Ground tracking requires an aerodynamically sensitive sphere because it is the relatively large total acceleration ($\frac{dv}{dt}$) which is measured rather than the relatively small drag acceleration ($g - \frac{dv}{dt}$) which is desired. Ground tracking, on the other hand, is required for the measurement of wind. Radar tracked inflated spheres having either a metallized surface or internal corner reflector constitute a very inexpensive sensor and payload but can be used only at radar sites. The most advanced radars permit measurement of density to perhaps 110 or 120 km and wind to 70 km.

DOVAP or other interferometer tracking requires electronics such as a transmitter or transponder in the sphere. The ground equipment is much simpler than radar, but the sphere electronics constitutes a penalty in weight and cost. Such spheres have been flown but are not in current use.

Internal accelerometers measure the drag acceleration directly and with great sensitivity. In one version an 18 cm diameter, 5 kg sphere containing an omnidirectional transit-time accelerometer measures density to about 100 km. See Fig. 1. Such a sphere is considerably more elaborate and expensive than a passive one but requires only telemetering and a balloonsonde ground facility. The most sensitive sphere system is one combining an inflatable envelope with internal accelerometers. (Faucher, et al 1967). The latter are tri-axis linear instruments which measure all components of acceleration. Such a sphere is shown in Fig. 2. Densities to altitudes of 140 km have been measured with this apparatus. Accelerometer spheres do

not measure wind although inertial reference systems for spheres which would measure wind have been suggested.

Refinements in sphere data processing have progressed with the development of payloads. The majority of the data reduction from spheres is now accomplished with computers. Many kinds of rockets have been used with spheres, the most popular being a single-stage 11.5 cm diameter solid propellant vehicle (ARCAS) which carries a radar tracked inflated sphere to 70 km, a two-stage solid propellant vehicle with 16 cm diameter second stage (Nike-Cajun) carrying either an inflated or a small rigid sphere to 150 km, and a two-stage solid propellant vehicle with 23 cm diameter second stage (Nike-Iroquois) carrying an instrumented inflatable sphere to nearly 200 km.

Inflatable, Radar-Tracked Spheres

During the IQSY a tabulation of sphere flights was made for COSPAR. In the period January 1964 to December 1965 experimenters in 10 laboratories carried out 170 flights of spheres of various kinds. In addition 113 flights were conducted by a U. S. Air Force contingent for operational purposes the sphere being of the inflatable, passive, radar-tracked type. Of the, 170 IQSY flights more specifically directed to atmospheric research, 154 were also of the radar-tracked type including a particularly significant southern hemisphere series of 45 launched by the Australians. The rest were launched by U. S. groups. The numerical preponderance of radar-tracked spheres is due, no doubt, to their reliability and very low cost. For the future, the use of this type is likely to increase with the proliferation of quality radar. Most of the following discussion will be devoted to the passive

inflated type with particular details relating to those used at Michigan. Rather complete descriptions with "how-to-do-it" details of nearly all types of spheres, including, those with accelerometers, are given in a COSPAR Technique Manual (Jones, ed. 1967) just issued.

Sensitivity to density and wind, being a function of the mass to area ratio, dictates the lightest possible envelope. Typically half-mil (0.0125 mm) Mylar is used. The inflation gas is isopentane. For a 66 cm sphere the weight breakdown is: sphere envelope 34 grams; isopentane, 8 grams; isopentane capsule, 8 grams.

Spheres are ejected in the aft direction in order to increase the separation from the rocket both by the ejection velocity and the force of drag. The ejection velocity is about 30 m/sec. Ejection usually takes place at 85 km which, for the Nike-Cajun is 70 seconds after take-off. A 66 cm sphere and inflating capsule are shown in Fig. 3. The details of the capsule are shown in Fig. 4. The acceleration of ejection, which is several km/sec^2, deflects the needle against a restraining spring. The needle pierces the diaphragm and the isopentane is released. The 8 grams of isopentane will inflate the spheres sufficiently for them to keep their shape above 14 mb or 29 km. Fig. 5 shows a sphere with its protective staves and the aluminum tube into which the sphere and staves are inserted. The tube is closed at the exit end with a bulkhead, riveted in place, and an aerodynamic fairing. At the other end is a black-powder operated gas-tight piston which upon firing with a squib, develops sufficient force to shear the rivets and eject the sphere. The piston remains in the ejector tube and prevents the ejection of hot gas and particles which might damage the sphere.

Data Analysis

In vector form the drag equation (1) is written

$$\overline{F_D} = -\tfrac{1}{2} \quad v\,\overline{v}\,C_D A \tag{3}$$

where $\overline{v}$ is the difference between the sphere velocity $\overline{v}$ and the wind $\overline{W}$.

$$\overline{v} = \overline{V} - \overline{W} \tag{4}$$

$$v = \left[(V_x - W_x)^2 + (V_y - W_y)^2 + (V_z - W_z)^2\right]^{\frac{1}{2}} \tag{5}$$

Under the assumption that there is no horizontal components of drag we have from Newton's law

$$\overline{F_D} = -m\,(\overline{g} + \overline{a}_b - \overline{a}) \tag{6}$$

where $\overline{a}_b$ is the acceleration due to buoyancy.

$$\overline{a}_b = -\,(\pi d^3/6m)\rho\,\overline{g} \tag{7}$$

d is the diameter and m the mass of the sphere.

Eliminating $\overline{F_D}$ and equating the vertical component of wind W_z to zero, four equations in four unknowns are obtained.

$$\rho = -2m\,(a_z + g - a_b) \,/\, C_D A v V_z \tag{8}$$

$$W_x = V_x - a_x V_z/(a_z + g - a_b) \tag{9}$$

$$W_y = V_y - a_y V_z/(a_z + g - a_b) \tag{10}$$

$$W_z = 0 \tag{11}$$

A vertical wind cannot be distinguished from a density gradient with a single sphere and must be ignored. Large-scale vertical wind is believed to be small (Kays and Craig, 1965). Vertical wind due to gravity waves is not easily estimated but may be significant (Witt, 1962) if strong waves are present.

Numerical differentiation of the radar data leads to the velocities and accelerations required in eqs. 8 to 11. Coriolis and centrifugal accelerations must also be introduced. The drag coefficient C_D as a function of Mach number and Reynolds number is obtained experimentally from wind tunnel and ballistic tunnel measurements on small spheres. Dimensional analysis and the general agreement with other methods confirm the essential correctness of scaling according to the Mach and Reynolds numbers. Improved measurements of C_D become available from time to time and reduce errors due to this coefficient.

Eqs. 8 to 11 are correct throughout but at high altitude the sensitivity to wind and the buoyancy are negligible. The equations of motion become

$$\rho = - 2m\,(a_z+g)/C_D A v V_z \qquad (12)$$

$$V = (V_x^2 + V_y^2 + V_z^2)^{\frac{1}{2}} \qquad (13)$$

$$W_x = W_y = W_z = 0 \qquad (14)$$

The ascending portion of the sphere trajectory is always at high altitude and is therefore measured by the nearly vertical radar range vector. In this case

$$\rho = -2m\,(a_r+g_r)/C_D A v V_r \qquad (15)$$

$$W = 0$$

Eq. 15 eliminates an important source of error because it is not necessary to numerically differentiate for the range rate which is a direct output of some advanced radars. Eq. (15) cannot be used on descent, however, because the density calculated will be sensitive to horizontal winds if the radar beam is not vertical.

In reducing the data, the highest acceptable point of the density profile is determined by fitting a straight line to eleven values of C_D which span

10 km. If any C_D falls more than 20% from the line, the process is repeated 1 km lower until the criterion is met. At 120 km the drag acceleration is about 1% of g and reliable results are unlikely above this altitude. This conclusion has been supported by simulation studies on an isothermal atmosphere with assumed radar errors. The data reduction process is computerized and the results for a typical flight are shown in Tables 1 and 2.

Performance, Errors, Problems

Several combinations of falling sphere designs and radar equipment have been used by different groups. These tests appear to define quite well the equipment needed to obtain the desired tracking accuracy.

Australian experimenters have used an FPS-16 radar at Woomera and a 2 meter metallized surface sphere. Sphere apogee is approximately 125 km but radar slant range is greater because the radar site is not near the launch pad. Tracking accuracy appears to be adequate.

Michigan experimenters have used a 0.66 meter metallized surface sphere at Kwajalein with the long range TRADEX radar. Later, the same size sphere was used at Wallops with the FPS-16 radar which is near the launch pad. It is usually possible to track continuously over an apogee of 150 km but accuracy near maximum slant range of 160 km is questionable. Recently dual tracks on the same sphere were obtained at Wallops using the FPS-16 and FPQ-6 radars. Radar performance was evaluated by comparing density profiles derived from tracking data from each radar. Good agreement was obtained on the ascent part of the trajectory and also on the descent part below 80 km. Descending, above 80 km, agreement was not good and the FPS-16 was considered unsatisfactory compared with the more

powerful and more accurate FPQ-6. The FPS-16 can be modified by adding pre-amplifiers which are likely to upgrade performance from marginal to satisfactory with the 0.66 meter sphere.

The Robin 1-meter sphere uses an internal corner reflector rather than a metallized surface and is normally tracked by an FPS-16 radar. Apogee is typically 70 km. Tracking with the MPS-19 radar has been attempted but its accuracy was considered unsatisfactory (Lenhard and Doody, 1963). In this case MPS-19 data was processed by techniques developed for FPS-16 data and results were scattered. This difficulty could be overcome by using more smoothing which would also decrease resolution. This approach did not appear promising, apparently, as it was not done.

The drag equation contains the drag coefficient and the air density as a product. The accuracy of the falling sphere as a density sensor is therefore no better than the accuracy of the available drag coefficient data. At high altitude, sphere drag data at supersonic Mach numbers and small Reynolds numbers are required, at low altitude, subsonic Mach numbers and larger Reynolds numbers prevail. Some of the values of drag coefficient as a function of Mach number and Reynolds have become available from the work of many experimenters over the years. In general these are now good enough for atmospheric measurements although differences of 5 to 10% do exist for the measurement of equivalent points by separate investigators. Peterson (1967) has summarized the literature and some of the problems relating to drag coefficient. Recent measurements by Heinrich, et al (1965) were designed to simulate the full Mach number and Reynolds number range of an inflatable falling sphere. When 0.66 meter falling sphere data was

Table 1. Computer Output, Typical Firing, Ascending Data

ALTITUDE KM	DENSITY KG/CU.M	TEMP K	PRESSURE MILLIBAR	CD	RE	MACH	KNUDSEN	SPEEDR	TOTVEL M/S	DELZ KM	XDB VAR
120.01	1.42 -8	361	1.47 -5	3.704	2.78-1	1.64	8.81	1.38	626.3	10.0	
119.00	1.57 -8	358	1.61 -5	3.637	3.17-1	1.69	7.94	1.41	641.1	9.4	.49
118.00	1.90 -8	327	1.78 -5	3.501	4.19-1	1.81	6.43	1.51	655.9	8.9	.52
117.03	2.40 -8	287	1.97 -5	3.341	5.99-1	1.97	4.91	1.65	669.9	8.4	.53
116.01	3.05 -8	256	2.23 -5	3.198	8.50-1	2.13	3.74	1.79	684.7	7.9	.45
114.99	3.71 -8	241	2.56 -5	3.102	1.11 0	2.24	3.02	1.88	698.7	7.4	.41
113.98	4.45 -8	231	2.95 -5	3.020	1.41 0	2.34	2.48	1.96	712.9	7.0	.48
112.97	5.34 -8	223	3.42 -5	2.948	1.76 0	2.42	2.05	2.03	726.0	6.6	.64
112.02	6.29 -8	218	3.94 -5	2.886	2.16 0	2.49	1.72	2.08	738.4	6.2	.75
111.02	7.46 -8	214	4.59 -5	2.824	2.65 0	2.56	1.44	2.14	752.7	5.9	.75
109.99	8.77 -8	214	5.38 -5	2.773	3.17 0	2.61	1.23	2.18	766.0	5.5	.53
109.01	1.02 -7	215	6.25 -5	2.728	3.72 0	2.65	1.06	2.21	777.6	5.2	.50
108.01	1.17 -7	216	7.29 -5	2.683	4.35 0	2.68	.92	2.24	791.0	4.9	.56
106.99	1.35 -7	219	8.52 -5	2.640	5.04 0	2.71	.80	2.27	804.9	4.6	.51
106.00	1.58 -7	218	9.90 -5	2.589	6.01 0	2.76	.68	2.31	817.4	4.3	.63
104.96	1.91 -7	212	1.16 -4	2.522	7.52 0	2.84	.56	2.37	829.8	4.1	.64
104.01	2.29 -7	206	1.35 -4	2.453	9.37 0	2.92	.47	2.44	842.0	3.9	.92
103.04	2.68 -7	206	1.58 -4	2.394	1.12 1	2.97	.40	2.49	855.7	3.6	.76
101.96	3.09 -7	211	1.87 -4	2.343	1.28 1	2.98	.35	2.49	868.8	3.4	.76
											.26

Table 2. Computer Output, Typical Firing, Ascending Data

ALTITUDE KM	DENSITY KG/CU.M	TEMP K	PRESSURE MILLIBAR	WINDS M/SEC SOUTH	WEST	TOTAL	CD	RE	MACH	TOTVEL M/S	TOTRV M/S	DELZ KM	XDB VAR
102.04	2.62 -7	221	1.66 -4				2.428	1.01 1	2.82	839.9		10.0	
100.99	3.59 -7	191	1.96 -4				2.265	1.58 1	3.07	850.9		10.0	1.25
100.02	4.39 -7	185	2.33 -4				2.163	2.01 1	3.14	857.9		10.0	1.20
98.98	5.83 -7	170	2.84 -4				1.988	2.91 1	3.31	865.7		10.0	.97
98.02	6.42 -7	184	3.39 -4				1.964	3.03 1	3.22	873.3		10.0	.78
96.99	8.08 -7	177	4.10 -4				1.834	3.94 1	3.29	879.2		10.0	.84
96.01	9.40 -7	182	4.92 -4				1.772	4.51 1	3.27	886.0		10.0	.71
94.98	1.19 -6	175	5.96 -4				1.667	5.96 1	3.36	892.1		10.0	.59
93.99	1.51 -6	167	7.22 -4				1.577	7.87 1	3.45	894.7		10.0	.58
93.01	1.88 -6	163	8.80 -4				1.509	1.00 2	3.50	897.2		10.0	.61
92.04	2.46 -6	153	1.08 -3				1.420	1.39 2	3.61	896.7		10.0	.50
90.97	3.09 -6	154	1.36 -3				1.368	1.75 2	3.60	895.8		10.0	.53
89.98	3.70 -6	158	1.68 -3				1.338	2.03 2	3.54	892.5		10.0	.55
89.01	4.30 -6	166	2.05 -3				1.322	2.26 2	3.44	886.4		9.4	1.07
87.97	5.02 -6	174	2.51 -3				1.307	2.50 2	3.32	877.5		8.8	1.23
87.02	5.69 -6	183	3.00 -3				1.297	2.67 2	3.20	867.0		8.4	1.26
85.98	6.42 -6	195	3.60 -3				1.290	2.81 2	3.05	853.8		7.9	1.21
84.98	7.37 -6	201	4.26 -3				1.276	3.09 2	2.96	840.0		7.4	1.19
83.99	8.60 -6	203	5.01 -3				1.261	3.49 2	2.87	821.0		7.0	.95
83.01	1.03 -5	200	5.89 -3				1.240	4.10 2	2.81	798.7		6.6	.93
81.99	1.26 -5	195	7.01 -3				1.215	4.96 2	2.76	773.1		6.2	1.01
81.01	1.55 -5	187	8.31 -3				1.193	6.09 2	2.71	743.5		5.8	.64
80.01	1.97 -5	177	9.99 -3				1.169	7.67 2	2.63	701.3		5.5	.73
78.99	2.41 -5	176	1.21 -2				1.152	8.80 2	2.45	652.2		5.2	.64
78.00	2.92 -5	175	1.47 -2				1.130	9.88 2	2.27	602.9		4.9	.53
76.98	3.51 -5	176	1.78 -2				1.110	1.06 3	2.04	542.4		4.6	.60
76.02	4.24 -5	176	2.13 -2				1.084	1.16 3	1.84	488.3		4.3	.50
75.00	4.90 -5	183	2.58 -2				1.052	1.13 3	1.58	427.3		4.1	.79
74.00	5.57 -5	192	3.08 -2				1.018	1.08 3	1.35	373.6		3.8	.73
73.00	6.20 -5	205	3.65 -2				.975	1.00 3	1.15	330.1		3.6	.74
72.01	6.83 -5	217	4.26 -2				.899	9.36 2	.99	293.9		3.4	.52
70.99	8.64 -5	202	5.01 -2				.725	1.15 3	.94	267.1		3.2	.86
70.00	1.03 -4	200	5.91 -2	-2.0	29.4	29.5	.635	1.32 3	.90	249.9	255.9	3.0	.82
69.01	1.24 -4	197	6.99 -2	-24.4	1.0	24.4	.576	1.45 3	.82	230.6	230.9	3.0	1.19
68.01	1.43 -4	201	8.27 -2	6.6	-2.4	7.0	.526	1.54 3	.76	215.1	215.2	3.0	.90
67.00	1.53 -4	221	9.71 -2	3.8	8.1	8.9	.504	1.49 3	.71	210.6	211.9	3.0	.81
66.01	1.69 -4	232	1.12 -1	-3.6	-32.7	32.9	.475	1.46 3	.64	194.5	195.2	3.0	.67
65.00	1.91 -4	236	1.30 -1	11.3	-17.5	20.9	.465	1.54 3	.60	182.9	184.1	3.0	1.01
64.00	2.19 -4	238	1.49 -1	-.9	59.1	59.1	.464	1.74 3	.59	175.4	183.2	3.0	.56
63.00	2.54 -4	237	1.72 -1	-7.2	44.5	45.1	.456	1.84 3	.54	166.0	166.9	3.0	.77
61.99	2.77 -4	249	1.98 -1	11.5	46.2	47.6	.450	1.86 3	.51	160.3	160.7	3.0	.31
61.00	3.09 -4	254	2.26 -1	-3.5	12.5	13.0	.444	1.92 3	.47	152.9	151.5	3.0	.17
60.00	3.38 -4	265	2.57 -1	-6.3	16.1	17.3	.441	1.90 3	.43	142.8	141.4	3.0	.21
59.00	3.81 -4	267	2.92 -1	19.8	7.3	21.1	.438	2.05 3	.42	136.0	136.2	3.0	.16
57.99	4.28 -4	269	3.31 -1	15.8	-3.1	16.1	.434	2.15 3	.39	127.6	127.7	3.0	.17
57.01	4.85 -4	269	3.74 -1	18.2	-.3	18.2	.433	2.26 3	.36	119.4	118.8	3.0	.29
56.00	5.37 -4	274	4.24 -1	9.6	-8.4	12.8	.432	2.34 3	.34	113.5	112.8	3.0	.28
55.00	5.83 -4	285	4.78 -1	7.8	-3.0	8.3	.432	2.35 3	.32	108.2	107.6	3.0	.32
54.00	6.46 -4	289	5.37 -1	-.4	-1.7	1.8	.431	2.44 3	.30	101.8	101.8	3.0	.32
53.00	7.22 -4	291	6.03 -1	-6.8	-7.3	9.9	.430	2.58 3	.28	96.9	97.1	3.0	.31
52.00	8.12 -4	291	6.77 -1	-1.8	-16.9	17.0	.429	2.74 3	.27	91.9	91.5	3.0	.32
51.00	9.34 -4	284	7.61 -1	6.1	-20.9	21.7	.427	3.00 3	.25	87.3	85.7	3.0	.39
50.00	1.06 -3	281	8.57 -1	6.2	-25.7	26.4	.427	3.14 3	.23	81.4	78.0	3.0	.36
49.00	1.21 -3	279	9.68 -1	.3	-28.2	28.2	.427	3.44 3	.22	78.8	74.5	3.0	.25
48.00	1.36 -3	279	1.09 0	-4.5	-22.3	22.7	.426	3.62 3	.21	73.9	69.8	3.0	.18
47.00	1.52 -3	282	1.23 0	-4.0	-19.7	20.1	.426	3.75 3	.19	68.7	65.3	3.0	.22
46.00	1.75 -3	276	1.39 0	1.5	-19.2	19.2	.427	4.22 3	.19	65.5	62.6	3.0	.29
45.00	1.93 -3	282	1.57 0	4.8	-22.2	22.7	.426	4.10 3	.17	60.2	56.0	3.0	.49
44.00	2.23 -3	276	1.77 0	2.4	-19.1	19.3	.429	4.81 3	.17	59.4	56.1	3.0	.84
43.00	2.43 -3	285	1.99 0	1.2	-21.8	21.9	.428	4.54 3	.15	54.2	49.8	3.0	.62
42.00	2.83 -3	277	2.25 0	-.2	-20.8	20.8	.432	5.33 3	.15	53.3	49.2	3.0	.54
41.00	3.17 -3	278	2.54 0	6.7	-23.7	24.7	.432	5.37 3	.13	50.2	44.3	3.0	1.09
40.00	3.76 -3	266	2.88 0	7.7	-22.6	23.9	.436	6.20 3	.13	48.0	41.7	3.0	.87
39.00	4.37 -3	261	3.27 0	2.9	-23.5	23.7	.438	6.53 3	.11	44.3	37.2	3.0	.38
38.00	5.15 -3	253	3.73 0	1.3	-20.9	20.9	.443	7.39 3	.11	40.9	34.8	3.0	.68
37.00	6.19 -3	241	4.28 0	6.1	-23.1	23.9	.449	8.46 3	.10	39.4	32.0	3.0	.82
36.00	7.07 -3	242	4.92 0	4.0	-31.9	32.2	.448	8.35 3	.09	42.0	27.6	3.0	.81
35.00	8.13 -3	242	5.65 0	-5.8	-33.2	33.7	.456	9.82 3	.09	43.8	28.3	3.0	1.09
34.00	9.37 -3	242	6.51 0	-8.0	-36.3	37.2	.457	1.01 4	.08	44.8	25.1	3.0	.80
33.00	1.16 -2	227	7.52 0	-1.8	-41.9	42.0	.463	1.15 4	.07	47.2	22.1	3.0	1.01
32.00	1.41 -2	217	8.76 0	4.1	-43.4	43.6	.469	1.32 4	.07	48.0	20.0	3.0	1.01

reduced, it was found that the use of the old measurements by Wieselsberger (1922) and Lunnon (1928) resulted in more credible atmospheric temperature near stratopause. An elementary explanation for poor agreement is that accurate measurements of drag force or stream conditions are difficult in a wind tunnel or ballistic range. Other explanations are possible. The state of flow about a sphere may be only marginally stable and may change under the influence of subtle factors such as sphere surface roughness or spin or support interference. If this is true the real problem may lie in producing the correct state of flow about a sphere rather than in making accurate measurements. If the state of flow about spheres falling through the atmosphere is essentially unpredictable then different sphere soundings cannot be compared which is a more serious problem than merely inaccurate drag data.

It may be feasible to control the spinning motion and also the boundary layer separation from the surface of an inflatable sphere if this proves to be necessary or desirable. The weight of the inflation gas capsule may be sufficient to orient the spin axis vertically if it is fastened to the envelope. One or more circular fences on the sphere surface near its equator may then perform the function of stabilizing the location of boundary layer separation.

This discussion of sphere drag is necessarily somewhat speculative. Hopefully sphere drag work now in progress will uncover answers to these questions.

Eq. (2) used to calculate temperature from a profile of density illustrates several points in a consideration of errors, some of which are common to all conversions of density to temperature. Already noted is the necessity for choosing T_o and the fact that an error due to the choice becomes

negligible in 15 km. In an isothermal atmosphere the error is reduced ϵ - fold for each scale height. Although the temperature data at highest altitude is not as accurate as elsewhere, it is published because valid trends can often be seen. Note also that density is in both the numerator and denominator. This causes errors in temperature due to certain kinds of drag coefficient errors to tend to cancel. If the C_D errors were monotonic for example, eq. (2) would actually yield smaller errors in temperature than density. If all C_D's were in error by a constant factor no temperature error would result.

It is no longer a problem to deploy and inflate a sphere without destroying it but on descent the sphere must collapse somewhere and the rather involved problem of how to cope is of current interest. The inflated sphere is a super pressure balloon with internal pressure maintained by a charge of inflation gas independent of ambient atmospheric pressure. As the sphere descends its differential pressure decreases toward zero at deflation altitude. At lower altitudes internal pressure is no longer constant but follows the ambient pressure as the sphere collapses into a shape of smaller volume. Since it is not possible to make a satisfactory estimate of the drag of the collapsed shape it is no longer useful as a density sensor. As a wind sensor the collapsed balloon appears to be quite satisfactory. Actual deflation altitude may be slightly different from design deflation altitude due to variations in ambient pressure or in temperature of inflation gas. Corrections for these variations are not made since they are believed to be both small and speculative.

As a first approximation one should reject density data obtained below the design altitude of deflation and also data from spheres that suffer catastrophic failure due to large tears occurring at the time of deployment. Experience has shown that a more careful analysis is required. Spheres rarely fail catastrophically. Under the most favorable conditions, however, it appears that in a third to a half of the flights small leaks occur which may permit loss of half the inflation gas in 10 to 15 minutes of flight. The data are adversely affected in two ways when small leaks occur. Actual deflation altitude is now higher than design deflation altitude. A reliable indication of deflation is therefore needed so that invalid data can be discounted. Premature deflation also implies the mass of the sphere system has been decreased by the mass of the gas lost through leakage. Since calculated atmospheric density is proportional to the assumed mass of the sphere system the effect of gas leakage is to cause indicated density to be erroneously high if corrections are not made. As a practical example the 0.66 meter sphere used by the authors has a gross mass of 50 grams of which 8 grams is isopentane inflation gas. The design altitude of deflation is 29 km where ambient pressure is 14 mb. If half the isopentane gas escaped through slow leaks the sphere would deflate at 34 km where ambient pressure is 7 mb. If no correction for lost gas is made the indicated density would be 50/46 of actual density or 9 percent high. At higher altitude the correction would be smaller and would depend on the assumed rate of leakage which is not constant but depends on internal pressure. Other experimenters use other sphere designs whose parameters are different but the same problem appears to be present and a correction of similar magnitude is required. Any falling sphere measurement of diurnal or seasonal density variation may give misleading results if sphere mass is not corrected.

Various assumptions are made to develop a technique for determining altitude of sphere deflation. Numerous sphere flights indicate an abrupt increase in sphere drag at the design altitude of deflation accompanied by the radar AGC (automatic gain control) becoming more irregular. The increase in sphere drag is more than 100 percent and can be seen on a plot of rate of descent vs altitude. When these two changes are first observed simultaneously they are assumed to indicate time of deflation. If a leak is indicated a mass correction is made which depends exponentially on the time subsequent to sphere deployment. The correction may not be exact because the criteria for deflation may indicate an advanced state of collapse rather than the onset of deflation and the assumed leak rate may not be accurate but it is believed the bulk of the error can be eliminated in this way.

Some questions concerning sphere behavior are yet to be resolved. All observations of sphere performance are indirect and consequently not as clear cut as desired. The AGC response of inflated spheres is always more or less irregular under the most favorable conditions such as free fall at high altitude. The sphere surface should be a uniformly good electrical conductor in order to obtain steady reflections of the radar pulses. The spheres are built up from 20 gores cut from aluminized Mylar. The adhesive used to fabricate the spheres insulates each gore from its neighbor. As seen by radar the sphere is quite different from the isotropic reflector desired. The relative orientation of the radar antenna axis, sphere geometry axis, and sphere spin axis, all influence the effectiveness of the sphere as a reflector of radar waves. Prior to the time the sphere is assumed to deflate a change in character of the AGC is sometimes observed which may or may not be accompanied by relatively small sphere accelerations. It

is assumed that such an event may be caused by spinning motion of a well inflated sphere which has been induced by aerodynamic forces. Although it is sometimes assumed that the aerodynamic force on a symetrical sphere must be entirely drag (axial) with no lift (lateral) component a number of experiments indicate the contrary (Murrow and Henry, 1965, MacCready and Williamson, 1965, Shafrir, 1965). The possibility that irregular lateral forces may be accompanied by variable drag force and spinning motion may be a reasonable hypothesis. It should be noted that some experimenters use an internal corner reflector rather than a metallized spherical surface. The characteristic AGC response of the corner reflector may be a better indicator of the spin state of the sphere.

The different sphere configurations and data processing techniques adopted by different experimenters are factors to be weighed when considering the complex problem of sphere behavior. Some experimenters assume sphere deflation occurs when vertical sphere accelerations of either sign indicate atmospheric structure that exceeds certain limits (Engler, 1965). Use of this criterion, (Engler's "lambda-check") implies that deflation can increase or decrease the drag, which is open to question. The possibility of a false indication of collapse is raised by the use of a constant time increment in the data processing that tends to amplify effects of radar error at low altitude. The radar measures a smaller change of range and angle at low altitude where rate of descent is smaller. A radar error larger than expected may therefore indicate normal flight at high altitude and collapse at a lower altitude, according to the lambda check. The possibility of false indications of collapse caused by peculiar aerodynamic behavior of the sphere, as well as unexpected atmospheric structure or wind response all contribute to a rather controversial question.

Coordinated Sphere, Grenade and Hasp Soundings

Comparison of results from nearly simultaneous firings of different techniques is of significant interest and several cases involving spheres are available. In a few cases a sphere has been substituted for the last grenade on NASA grenade flights. Figures 6, 7, and 8, show a coordinated group of three sphere soundings, three grenade soundings, and four lower altitude Hasp soundings in a sixteen hour period in August 1965 at Wallops Island (38°N, 75°W). These simultaneous soundings and another group in October permitted an analysis of system performance that was of mutual benefit. Initially a considerable difference was found between zonal wind components indicated by sphere and by grenades. The sphere also indicated considerably higher temperature near the stratopause. A review of analyses of grenade data disclosed certain corrections are required which depend on ambient temperature near the microphone arrays. These corrections were more critical at Wallops due to the geometrical relationship between the rocket trajectory and the array of microphones. The corrections brought the wind measurements into agreement and decreased the temperature differences. A review of sphere drag measurements disclosed conflicting results reported by different experimenters. A choice of sphere drag data believed to be more accurate reduced sphere indicated temperature by about 12° K near stratopause, improving the agreement with grenades which is now good in most cases.

The Hasp system includes a thermistor temperature sensor. Wind data is also provided by a radar track of its parachute. Figure 6 shows the coordination of the August 7 and 8 soundings. Two of the Nike-Cajun rockets

carried a sphere only and data were obtained on the ascent as well as the descent parts of the trajectory. Three Nike-Cajun rockets each carried a payload of eleven grenades and also an inflatable falling sphere. It was necessary to delay the sphere deployment until all grenades were exploded, consequently no sphere data were obtained during ascent in this configuration. Grenade fragments apparently pierced the sphere envelope in two of these flights, the third was successful. An early evening sounding, Figure 7, compares sphere and grenade data nearly simultaneous in time, the grenade measurements precede the lower sphere measurements by 10 minutes at most. The wind data agree quite well at most points. Exact agreement should not be expected because the grenade data represents average values over 5 to 6 km. Grenades and sphere both indicate large wind shear and reversals near 70 km. Measurements of sphere drag by Wieselsberger (1922) and Lunnon (1928) were used to compute atmospheric density rather than the more recent measurements by Heinrich et al (1965). The temperature profile, Figure 7, shows quite good agreement between grenades and sphere at all levels. Below 55 km the temperature and density profiles indicated by the sphere exhibit a peculiar wave effect. This early night sounding was preceded in the afternoon and followed late at night by sphere and grenade soundings that were not simultaneous but separated by about 1 $\frac{1}{2}$ hours, Figures 8 and 9. The wind profiles obtained by the two techniques do not agree as well as in the simultaneous soundings, possibly due to a variable wind condition. The temperature data agrees quite well with two exceptions. At 78 km, Fig. 8, a grenade temperature may be abnormal. At stratopause, Fig. 9, the temperature according to spheres appears to be quite high. Below 55 km the wave like appearance of temperature and density

profiles indicated by spheres is very strong in the afternoon case and is less strong in the late night case, which terminates at 38 km. More low altitude data might have revealed more of the wave, however. The grenade data neither confirms nor denies these waves, a closer spacing between grenades would be required to make such a determination. The Hasp temperature data, Fig. 8 , is quite clear cut, however. It shows no waves and indicates strongly that the sphere data is erroneous.

Four explanations for the peculiar behavior of this sphere are logically possible: a poor radar track, a deflated sphere, peculiar aerodynamics of spheres, and vertical motion in the atmosphere. Incorrect sphere drag data is not a possible explanation, assuming a unique drag function exists, because such errors would influence all soundings in the same way. This sphere was dual tracked by the FPQ-6 and FPS-16 radars. A comparison of atmospheric density and temperature profiles derived independently from each track confirmed that accurate tracking was obtained in the altitude range in question. The evidence indicates that the sphere remained inflated down to 29 km where it was expected to deflate. Its rate of descent plot shows a sharp increase of drag at 29 km which suggests deflation. The radar AGC shows no indication of deflation at higher altitude and confirms deflation at 29 km by an abrupt change to an irregular pattern.

The peculiar aerodynamics of blunt bodies may cause the drag to be variable. The point at which the boundary layer separates from the sphere may be unstable. Any movement of the separation point can be expected to influence the pressure distribution, the wake, and the drag force. Instability may occur only in a certain range of Reynolds number and may be a function

of sphere rotation and surface roughness. If flow about the sphere oscillated between two states of marginal stability it might cause the wavelike profiles of Fig. 8 . A difficulty of this theory is to explain how a nicely formed wave is developed rather than a more random effect. Another difficulty is to explain why numerous sphere soundings appear to be free of this anomalous behavior.

Another explanation is based on the sensitivity of light weight spheres to vertical motions of the atmosphere which may be present during some flights but not others. This theory requires a large vertical wind component, about 3 m/s. Kays and Craig (1965) have estimated that large scale vertical motion in the upper stratosphere is of the order of 1 cm/s. The possibility of vertical motion induced by gravity waves should also be considered. Witt (1962) has estimated vertical wind as high as 25 m/s from noctilucent cloud observations above 80 km. Hines (private communication 1967) points out that short period gravity waves may induce relatively large vertical velocity. While 3 m/s may be above average for stratospheric vertical wind it does not appear to be out of the question.

To summarize, the analysis of coordinated sphere, grenade and Hasp soundings shows generally good agreement in wind, agreement between spheres and grenades in mesospheric temperature, and an oscillation in sphere-measured stratospheric temperature about the smoother mean of the Hasp experiment. Whether these oscillations are aerodynamic or atmospheric is unknown.

One of the most interesting comparisons of density from a sphere with density from another method comes from nearly simultnaeous flights at Wallops in 1963. The other experiment was a neutral mass spectrometer of the quadrupole type flown by Schaefer. Fig. 10 shows the result.

On another occasion a sphere was fired simultaneously with a vertical test of the San Marco drag satellite instrumentation and reasonable agreement was obtained.

Summary of Performance

The foregoing developments and problems are currently at the fore in sphere work and additional work is needed. With careful attention to detail, errors may be within the requirements of useful geophysical measurements. In Table 3 are summarized the ranges and estimates of errors of measurement for current practice with a 0.66 meter sphere and the best radar.

Table 3

	Altitude km	Error	Altitude km	Error	Altitude km	Error
Density	30-70	5%	70-105	5%	105-120	10%
Temperature	30-70	5%	70-105	5%	105-120	trends only
Wind, Magnitude	30-70	3 m/s				

Note: At Mach 1, in the vicinity of 70 km, density and temperature errors probably exceed the values shown.

Results

A principal contribution of spheres from the beginning has been that of providing profiles of density and temperature to model atmospheres including CIRA and the U. S. Standard and Supplemental. Observations by Faire and Champion (1965) and the present authors (Jones et al 1959; Peterson and McWatters, 1964) are in these models. CIRA 1965 is based in part on density measurements to nearly 150 km with the inflated accelerometer sphere of Faucher et al (1963). In contrast to these contributions there is to our knowledge no instance of an atmospheric structural phenomenon having been investigated on a global scale through the coordinated efforts of separate sphere investigators. We have cooperated better than this with the users of other techniques! In view of the low cost and ease of firing of inflated spheres it would seem that coordinated firings would be straightforward and perhaps it requires only that the effort be made. Series of sphere firings by single groups, on the other hand, have been quite successful in scanning various phenomena. These events include a latitude survey in 1956 and a fortuitous bracketing of an arctic explosive warning during IGY. (Jones et al, 1959). During IQSY Peterson et al (1965) carried out a comprehensive survey of the tropical Pacific atmosphere with a series of thirteen firings at Kwajalein. Fig. 11 shows average and extreme values of density, temperature and winds derived from the individual firings. The structure of the tropical upper atmosphere is confirmed to be subject to only small variations. Tropical models should perhaps show a 20% increase in density near 60 km compared with the U. S. Standard for 15^{o} N. The stratopause region is being reviewed in the light of new C_D values.

A series of inflated spheres (ROBIN) launched by the Air Force at Eglin, Florida in May 1961 and October 1962 was used by Webb (1964) in an analysis of stratospheric circulation. Fig. 12 shows zonal wind profiles from these flights. From these data Webb (1965) deduced the vertical scale of the wave structure of the vertical component and found suitable agreement with the meteor-derived vertical scales of Greenhow and Neufeld (1959). See Fig. 13.

Several attempts have been made to see in the mesophere and lower thermosphere the systematic density bulge of higher altitudes. Greenhow and Hall (1960) have done so at 96 km with two treatments of meteor observations. Fig. 14. A search for this feature in sphere data by Peterson and McWatters (1967) showed less heating and a more complex structure. Appropriate pairs of firings from the Kwajalein series (2 flights) and Wallops (7 flights), most of which were tracked with the best radar, were used in the study. Fig. 15 shows the diurnal variation for these pairs with the local times of firings indicated. Fig. 16 shows the average diurnal variation compared with the 96 km point of Greenhow and Hall. The sphere variation is at most half that indicated by meteors. The time resolution of two firings is poor, and maxima and minima may have been missed. The irregularities of the density variations apparent in Fig. 15 may result from the fact that heating in the region of the mesopause is more complex than at satellite altitudes. Possible energy sources are ozonospheres heating the energy of gravity waves which according to Hines (1960) can be deposited at the mesopause or higher, and the recombination of atomic oxygen postulated by Kellogg (1961) for polar regions which may be appropriate here. The latter phenomenon is suspected of large variations following the shifts from molecular to eddy

diffusion in a varying turbopause discussed by Johnson (1967) and Blamont (1967).

Observations with spheres by investigators of the Weapons Research Establishment and the University of Adelaide in Australia have been made on a truly comprehensive scale. During IQSY 45 firings were conducted. Of these, 10 were launched in a 24 hour period at Carnarvon, 25^{o} S. The others were at Woomera 31^{o} S. Pearson (1966) has analyzed the Woomera firings for density and temperature variations in a one year period March 1964 to March 1965. He includes also comparisons with grenade temperature profiles at Woomera showing reasonably good agreement. Rofe, et al (1967) (1966) have analyzed density and temperature results for the Carnarvon shots and in addition have summarized stratospheric and mesospheric circulation for Australia using both series. In contrast to astronomy, upper air structure in the southern hemisphere is rather well observed.

In summary, sphere investigations continue actively. Low cost and reliability together with new radars should increase the method's usefulness. Improved techniques and drag coefficients have reduced errors. Possible anomalous aerodynamic behavior in the stratosphere needs investigation. Profiles for models, comparisons with other methods, circulation models, diurnal and seasonal variations in density and temperature and mesopause dynamics have been the principal areas to which contributions have been made. Coordination among investigators for global scale measurements has been neglected and should be promoted.

References

Blamont, J. (private communication) 1967.

Faucher, G. A., J. F Morrisey and C. N. Stark, Falling sphere density measurements, J. Geophys. Res., 72, 299-305, 1967.

Faucher, G. A., R. W. Procunier, and F. S. Sherman, Upper-atmosphere density obtained from measurements of drag on a falling sphere, J. Geophys. Res., 68, 3437-3450, 1963.

Faire, A. C. and K. S. W. Champion, Falling sphere measurements of atmospheric density, temperature and pressure up to 115 km. Space Research V, King-Hele et al, eds., John Wiley and Sons, New York, 1039-1057, 1965.

Heinrich, H. G., E. L. Haak, and R. J. Niccum, Modification of the robin meteorological balloon: drag evaluation, University of Minnesota Final Report AF 19 (628) - 2945, AFCRL 65-734, Vol. II, 1965.

Hines, C. O., Internal atmospheric gravity waves at ionospheric heights, Can. J. Phys. 38, 1441 1481, 1960.

Johnson, F. S., Turbopause processes and effects, Space Research VII, R. L. Smith-Rose, ed., North Holland Publ. Co., Amsterdam, 262-269, 1967.

Jones, L. M. (ed) Falling sphere method for upper-air density, temperature and wind, COSPAR Technique Manual Series, Paris, 1967.

Jones, L. M., J. W. Peterson, E. J. Schaefer and H. F. Schulte, Upper-air density and temperature: some variations and an abrupt warming in the mesosphere, J. Geophys. Res. 64, 2231-2340, 1959.

Kays, M. and R. A. Craig, On the order of magnitude of large-scale vertical motions in the upper stratosphere, J. Geophys. Res., 70, 4453-4461, 1965.

Kellogg, W. W., Chemical heating above the polar mesopause in winter, J. Meteor., 18, 373-381, 1961.

Lenhard, R. W., and M. P. Doody, Accuracy of meteorological data obtained by tracking the ROBIN with MPS-19 radar, Instrumentation for Geophysics and Astrophysics 35, AFCRL-63-938, 1963.

Lunnon, R. G., Fluid resistance to moving spheres, Proc. Roy. Soc. (London) Series A, 118, 680-694, 1928.

MacCready, P. B., and R. E. Williamson, The motion of ascending and descending spheres, NASA CR-61102, 1965.

Murrow, H. N. and R. M. Henry, Self-induced balloon motions, J. Appl. Meteorol. 4, 131-138, 1965.

Pearson, P. H. O., Seasonal variations of density, temperature and pressure between 40 and 90 km, Woomera, South Australia, March 1964-March 1965, J. Atmos. Terr. Phys. 28, 1057-1064, 1966.

Peterson, J. W., in Appendix 7, Falling sphere method for upper-air density, temperature and wind, edited by L. M. Jones, COSPAR Technique Manual Series, Paris, 1967.

Peterson, J. W., W. H. Hansen, K. D. McWatters and G. Bonfanti, Falling sphere measurements over Kwajalein, J. Geophys. Res., 70, 4477-4489, 1965.

Peterson, J. W. and K. D. McWatters, Diurnal density variations near the mesopause, Proceedings AGU, Washington, D. C., 1967.

Peterson, J. W. and K. D. McWatters, The measurements of upper air density and temperature by two radar-tracked falling spheres, Univ. of Michigan, NASA Contr. Report 29, 1964.

Rofe, B., W. G. Elford and E. M. Doyle, Daily variations in winds, density, temperature and pressure between 40 and 90 km, in the subtropical latitudes of the southern hemisphere, Space Research VII, R. L. Smith-Rose, ed., North Holland Publ. Co., Amsterdam, 974-5, 1967.

Shafrir, V., Horizontal oscillations of falling spheres, Air Force Cambridge Research Laboratories, Report AFCRL-65-141, 1965.

Webb, W. L., Scale of stratospheric detail structure, Space Research V, King-Hele et al, eds., John Wiley & Sons, New York, 997-1010, 1965.

Wieselsberger, C., Weitere feststellringen uber die gesetze des flussigkeits und luftwinderstandes, Physik. Zeitschr. 23, 219-224, 1922.

Witt, G., Height, Structure and displacements of noctilucent clouds, Tellus, 14, 1-18, 1962.

LIST OF FIGURES

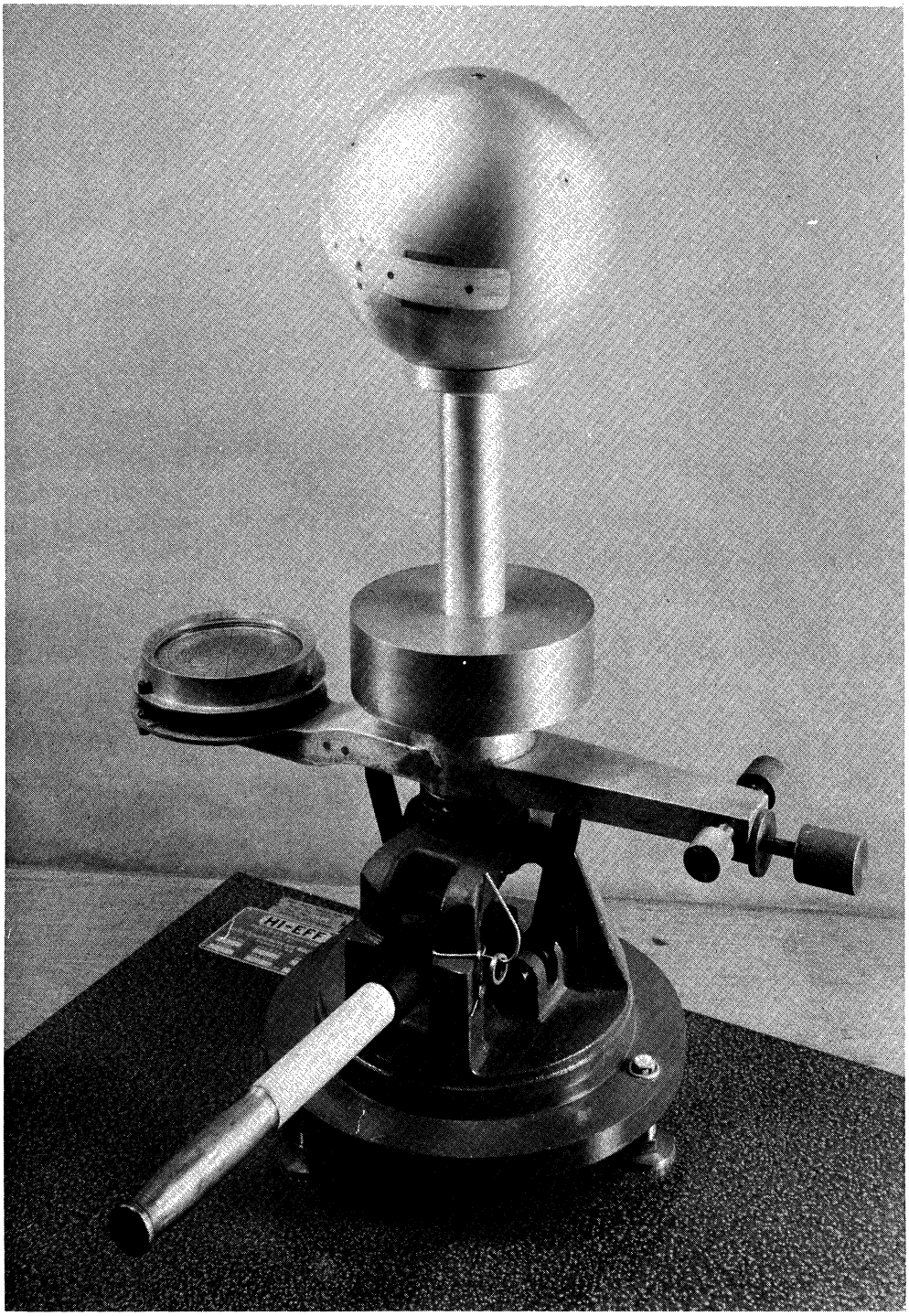

Fig. 1. Rigid 18 cm sphere with omni-directional accelerometer, University of Michigan.

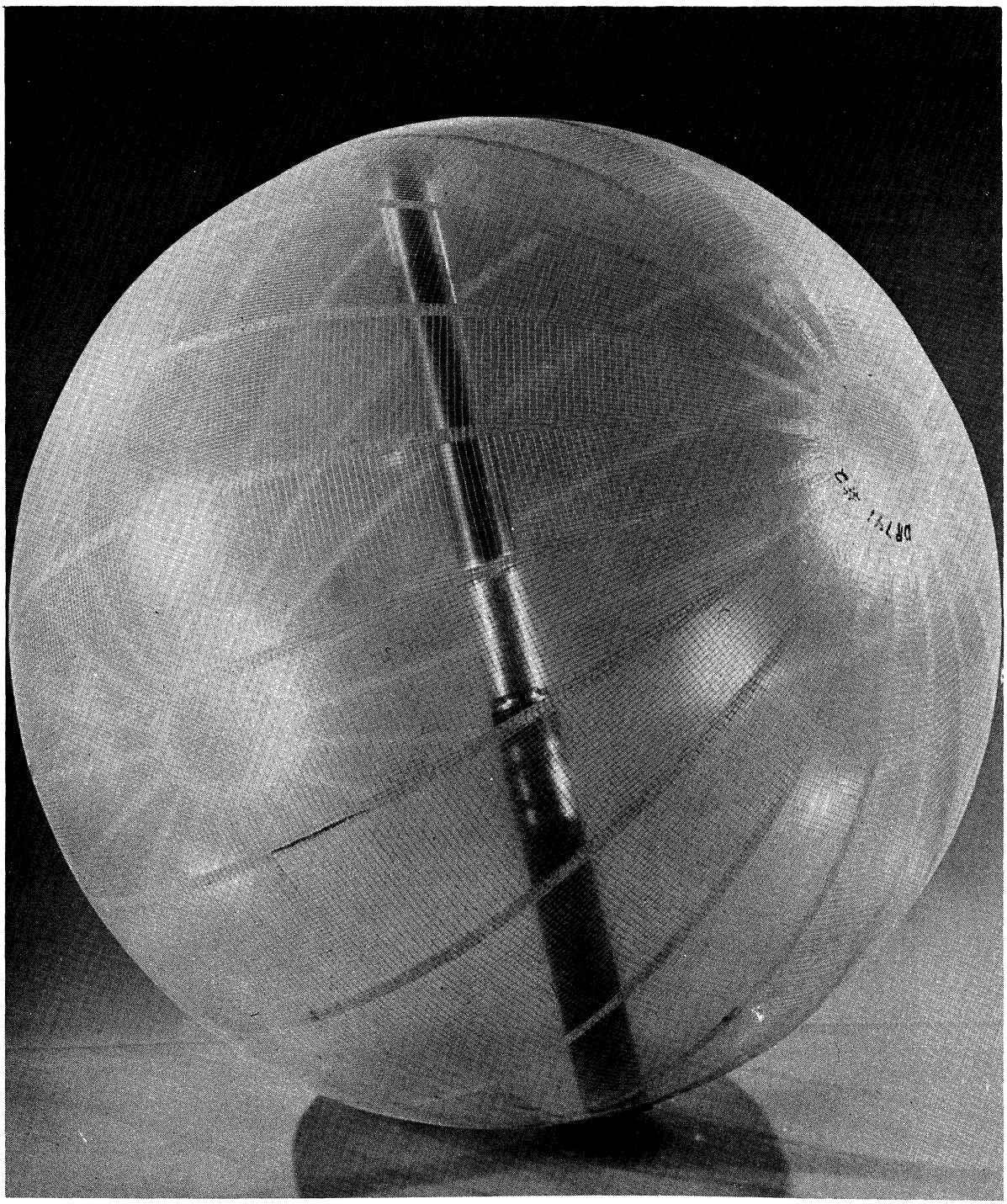

Fig. 2. Inflated 1 meter sphere with tri-axis accelerometers, AFCRL.

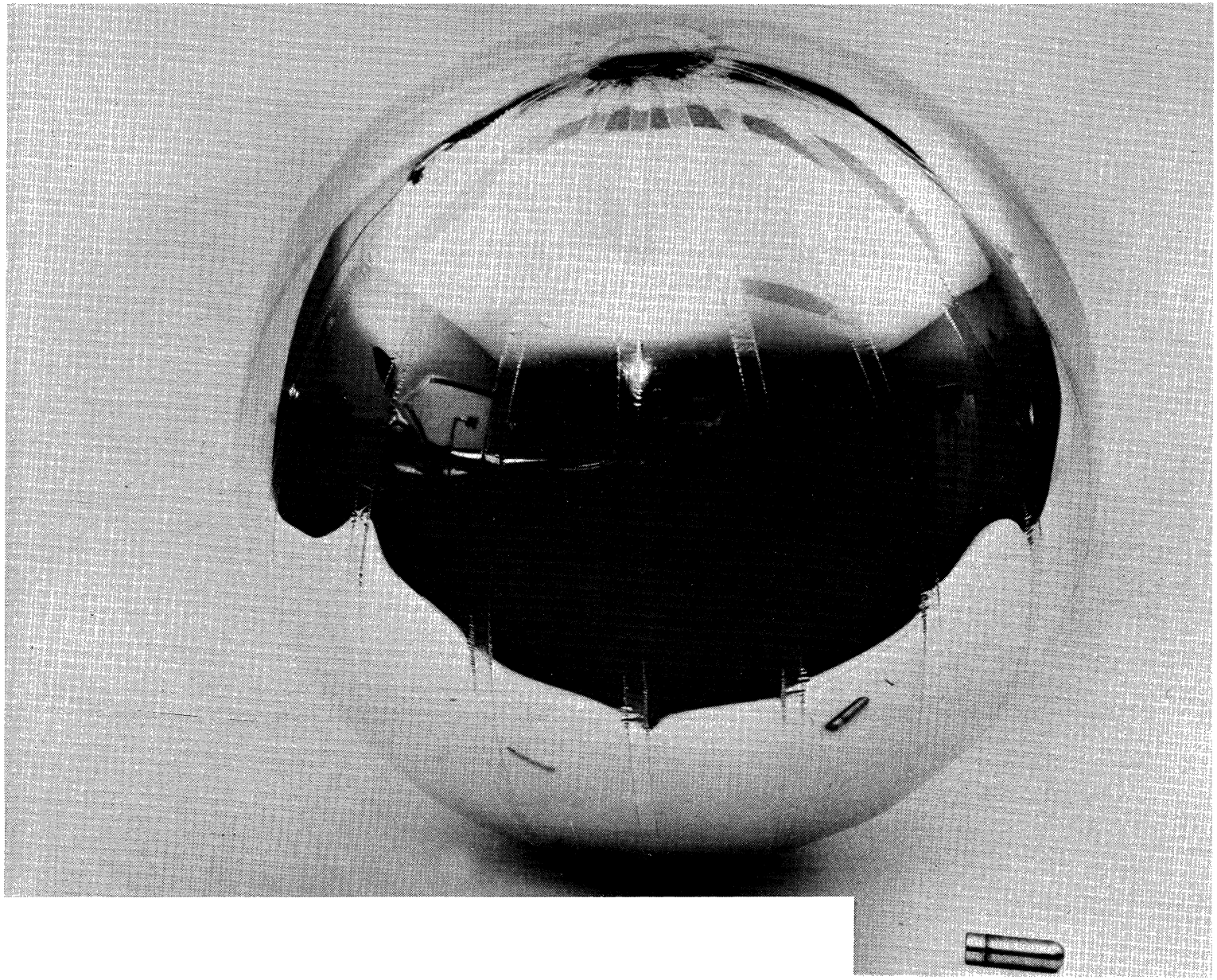

Fig. 3. Inflated, passive 66 cm sphere with isopentane capsule. University of Michigan.

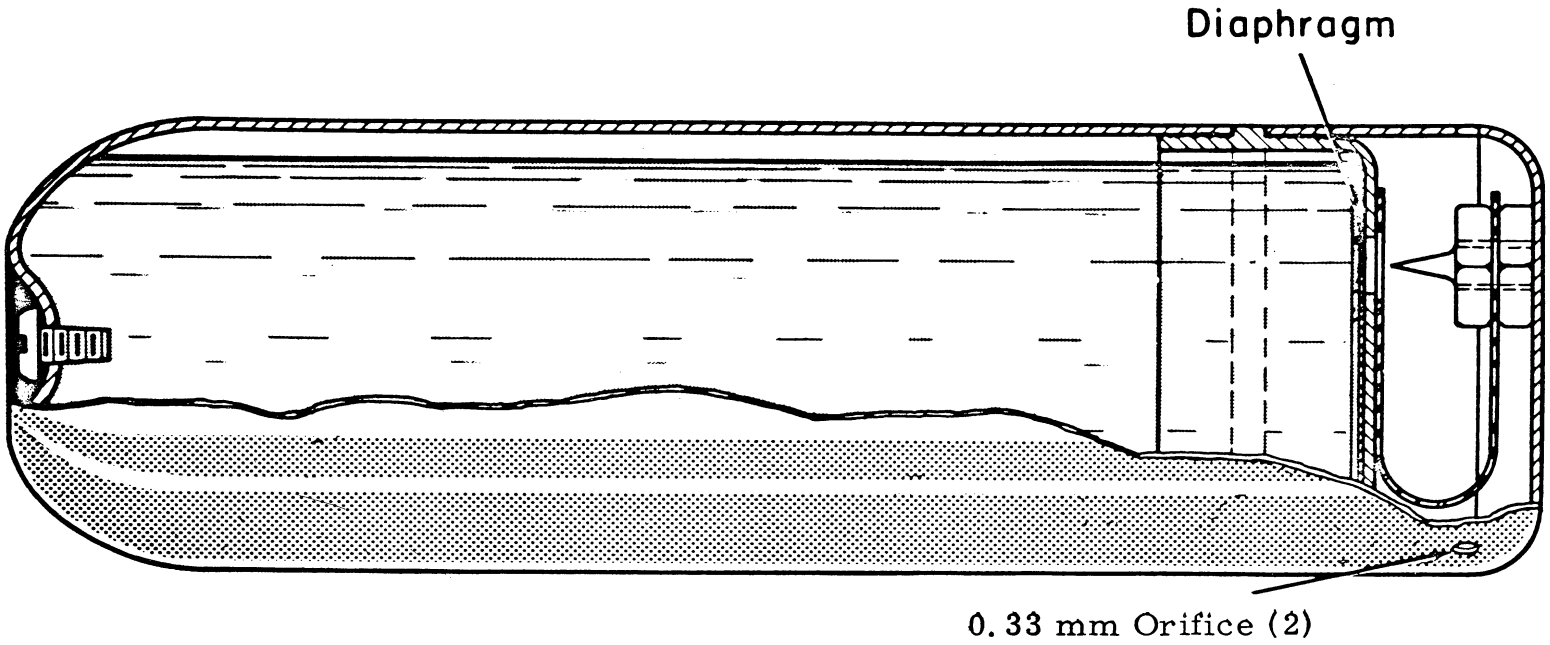

Fig. 4. Details of isopentane capsule.

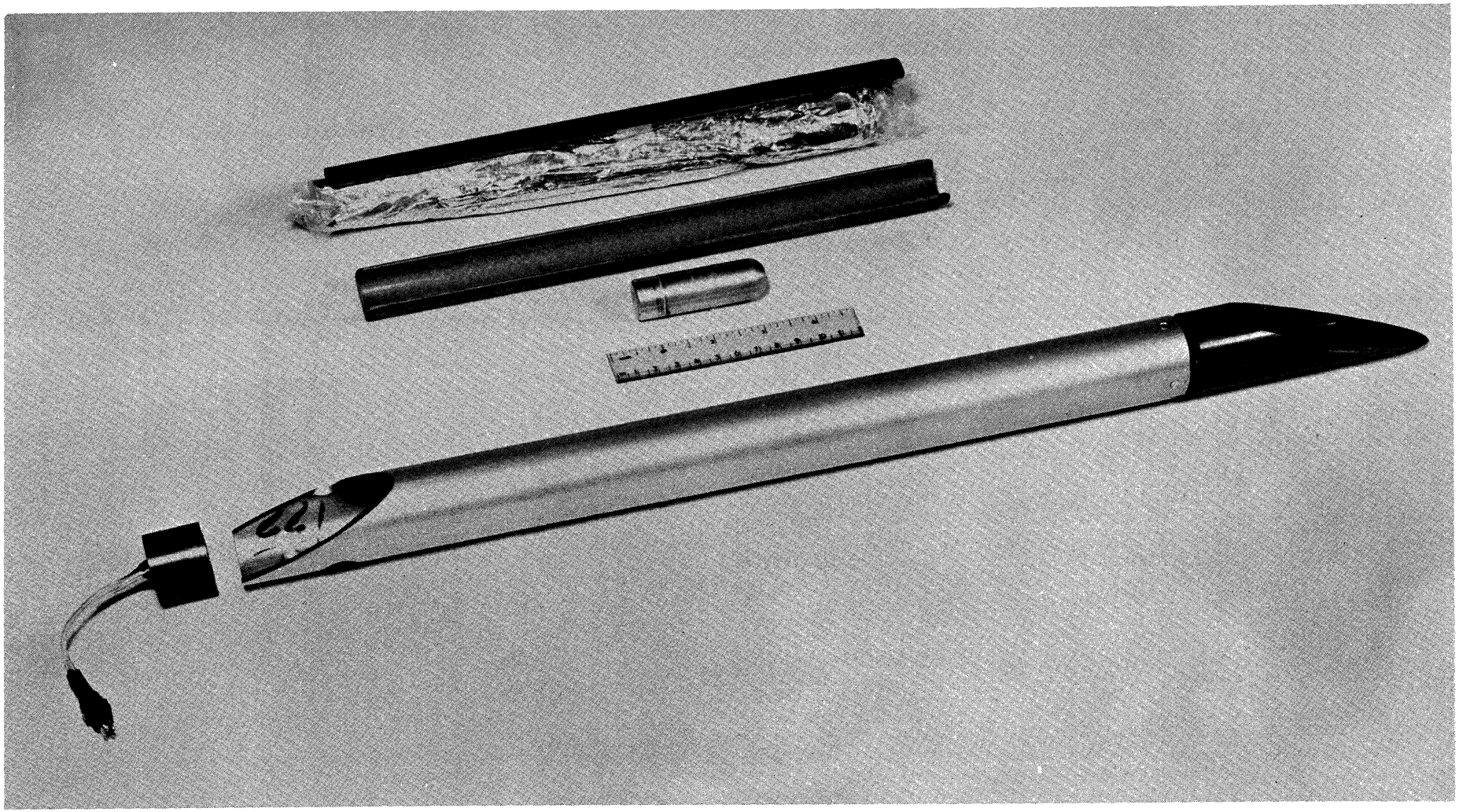

Fig. 5. Sphere, staves and capsule. Assembled tube with ejector and fairing.

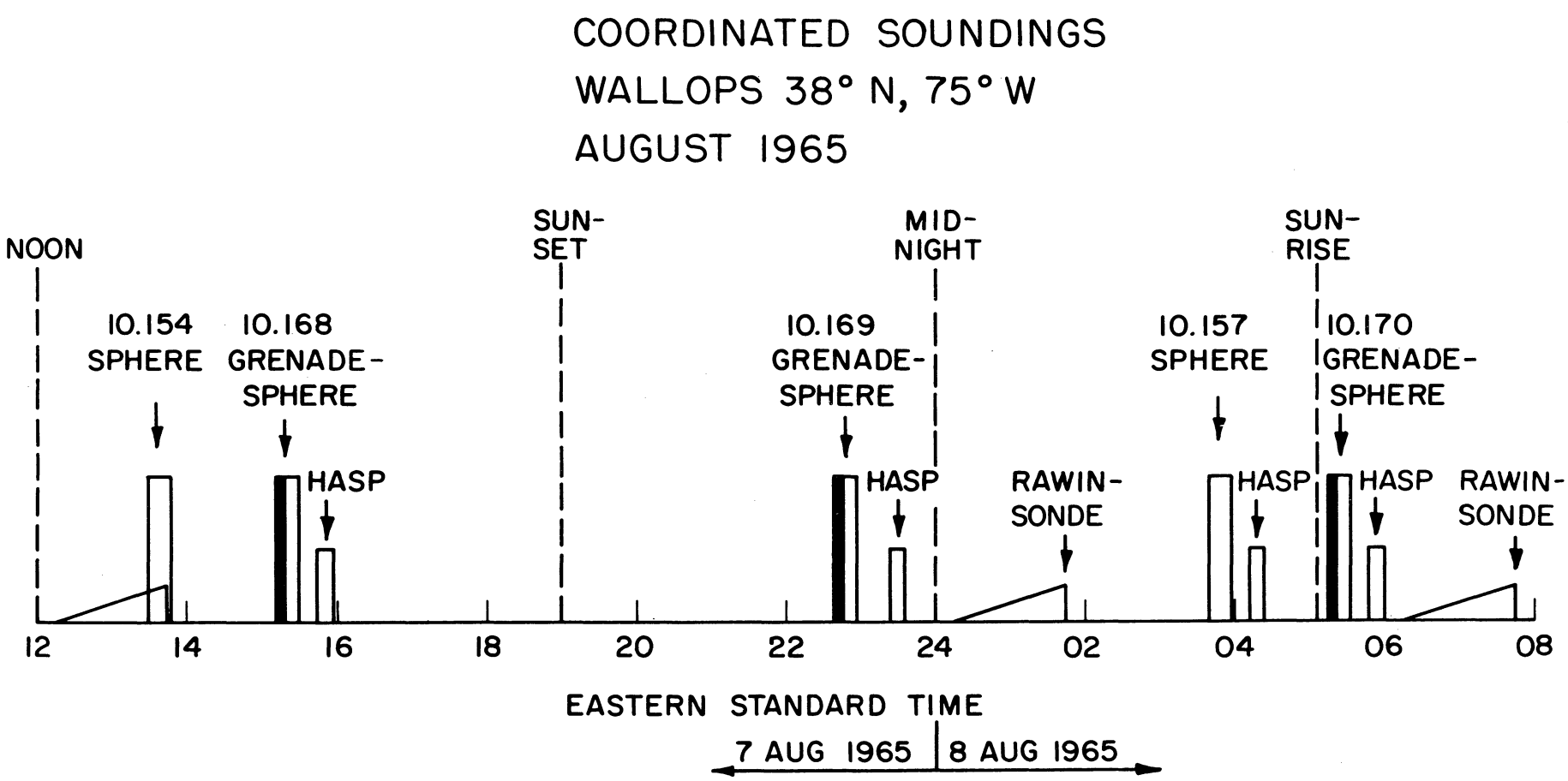

Fig. 6. Schedule of coordinated soundings at Wallops Island, 38° N, August 1965.

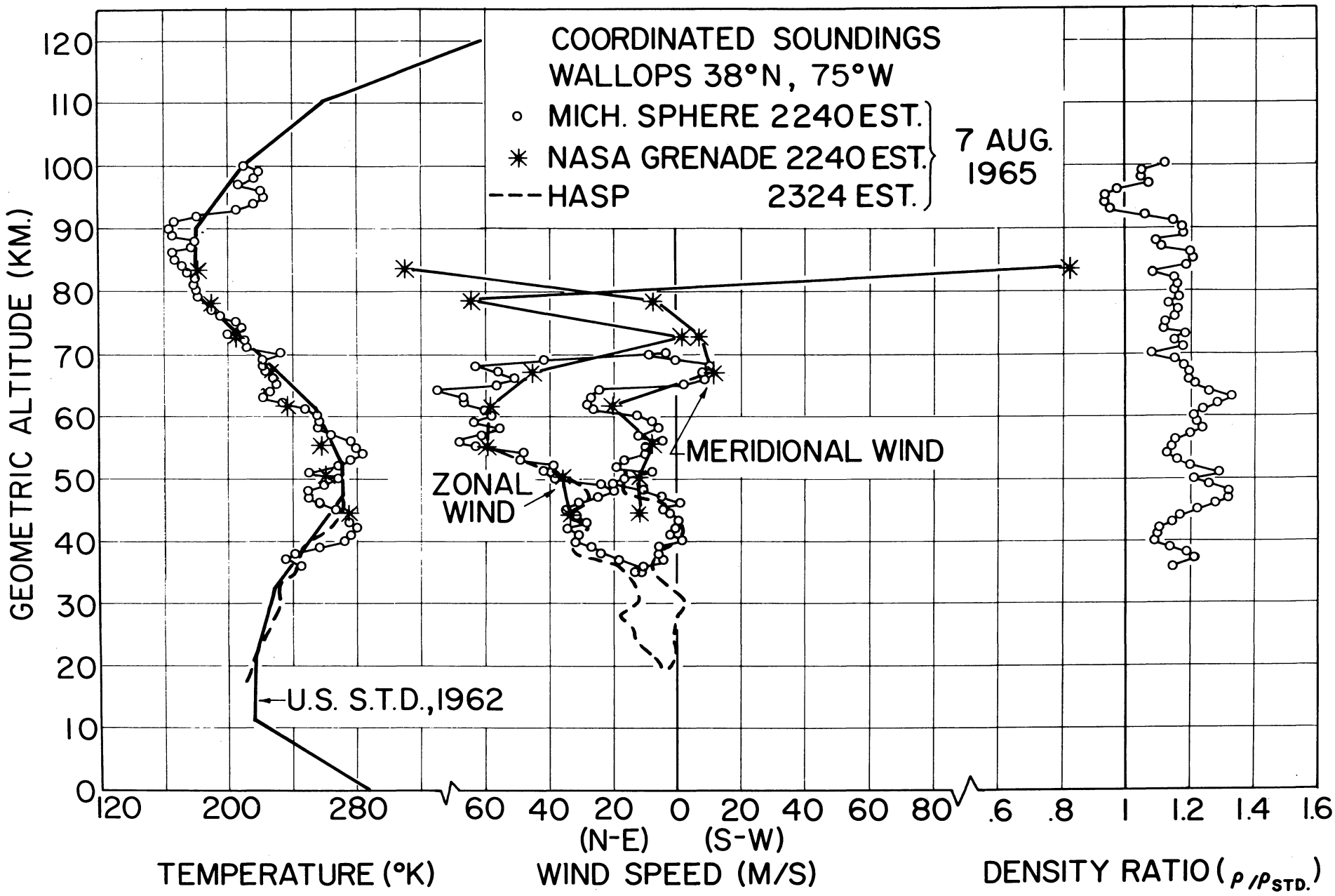

Fig. 7. Coordinated sphere, grenade and Hasp soundings: summer night, 1965.

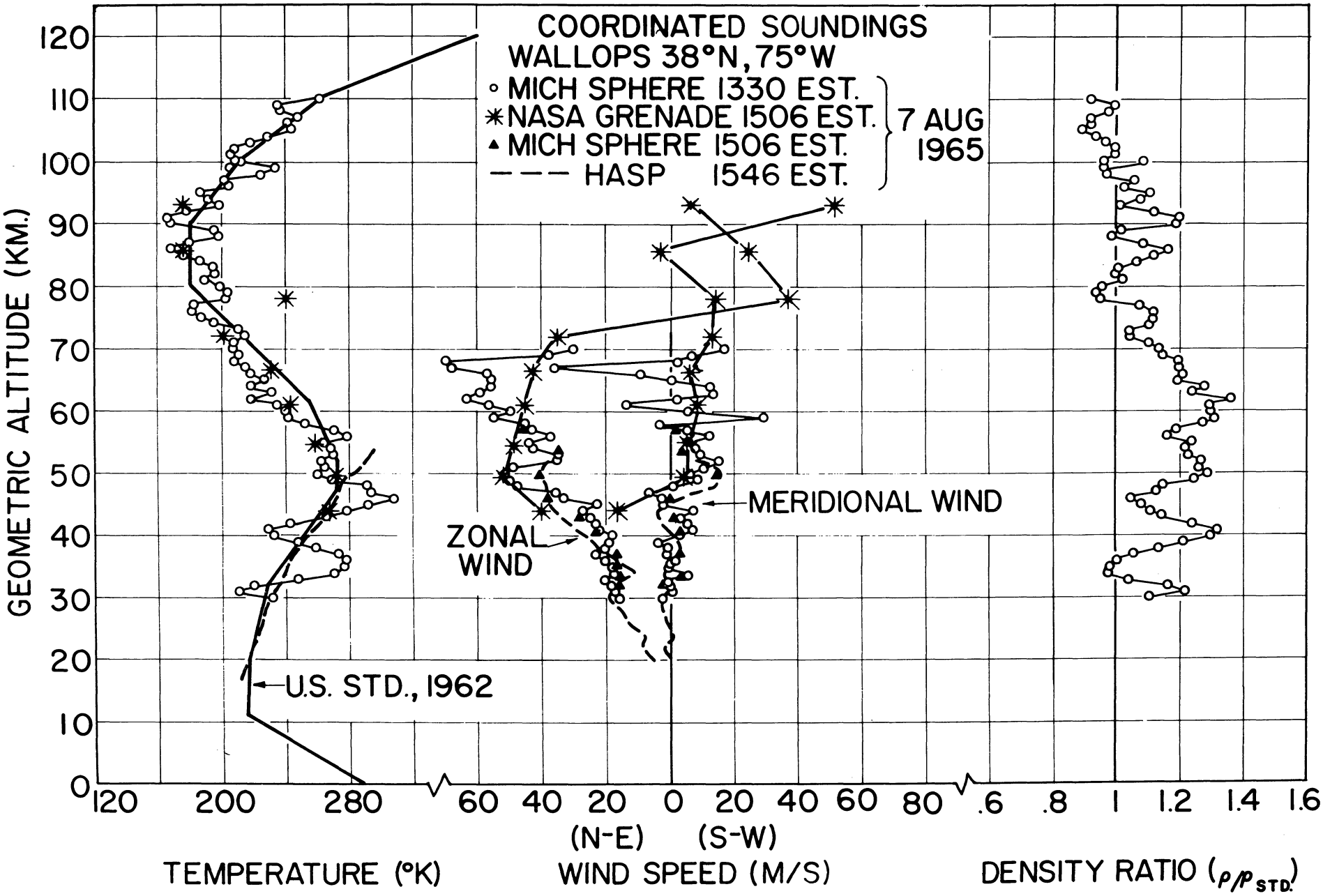

Fig. 8. Coordinated sphere, grenade and Hasp soundings: summer afternoon, 1965.

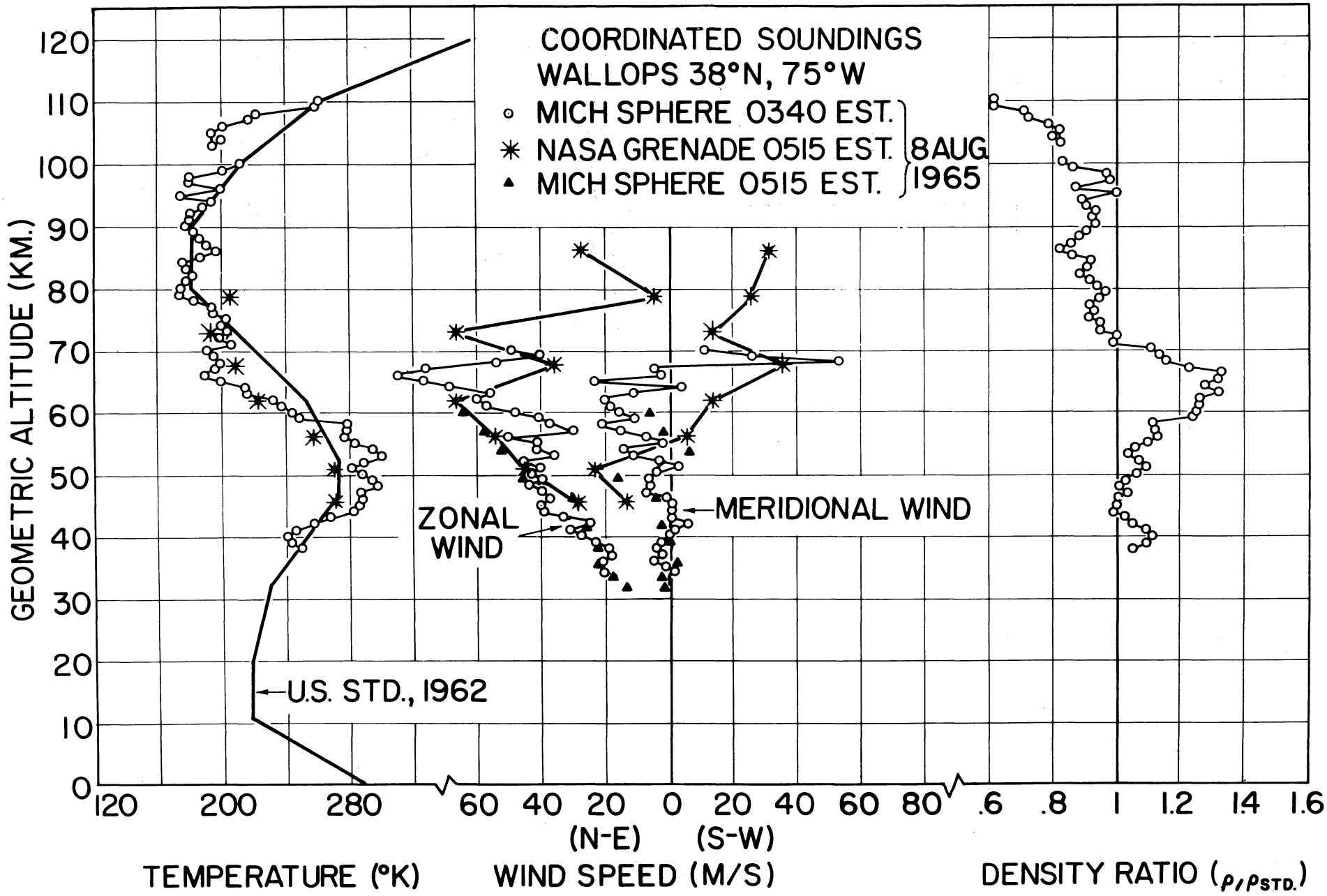

Fig. 9. Coordinated sphere and grenade soundings: summer early morning, 1965.

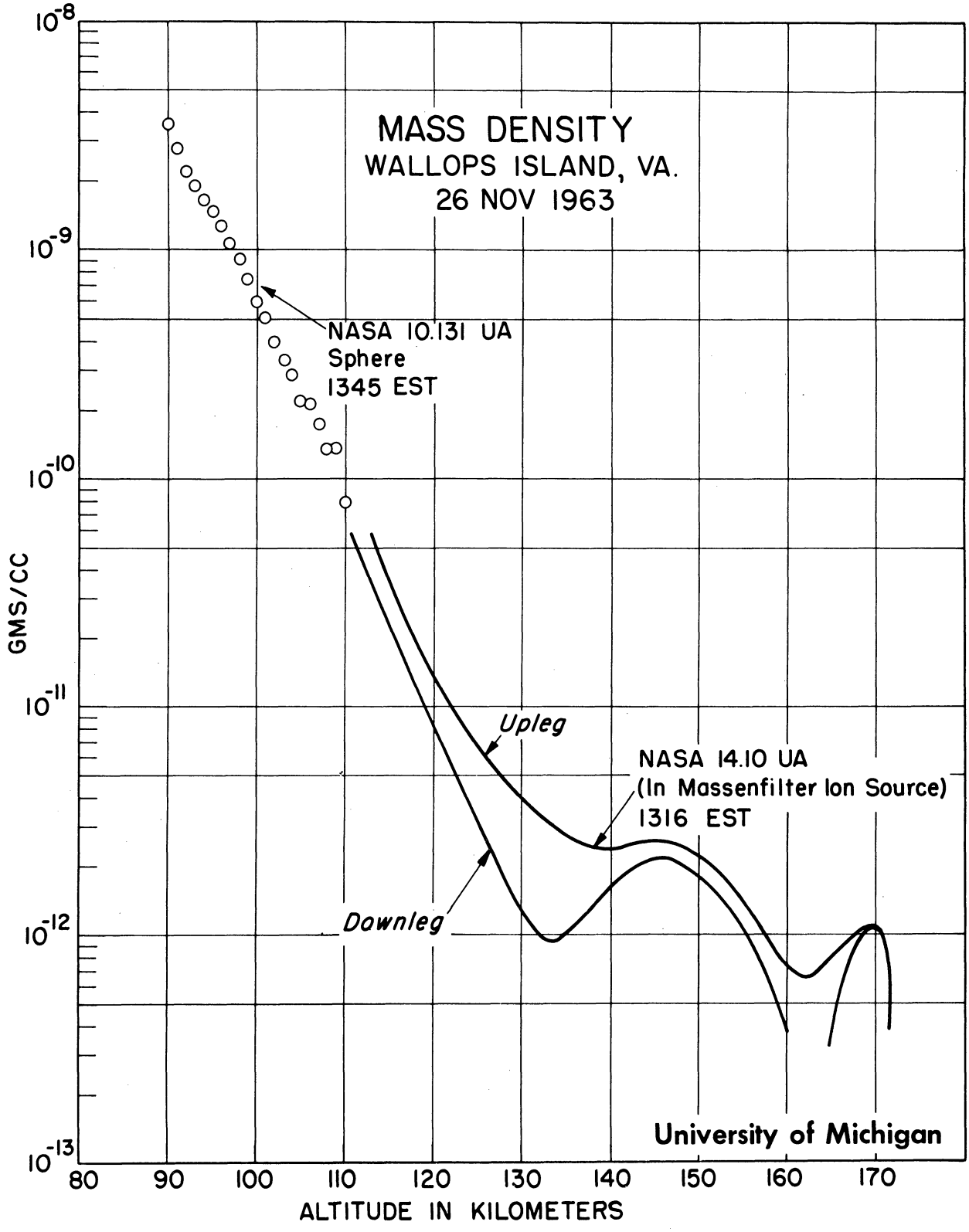

Fig. 10. Mass density measured by sphere and quadrupole mass spectrometer, 26 November 1963.

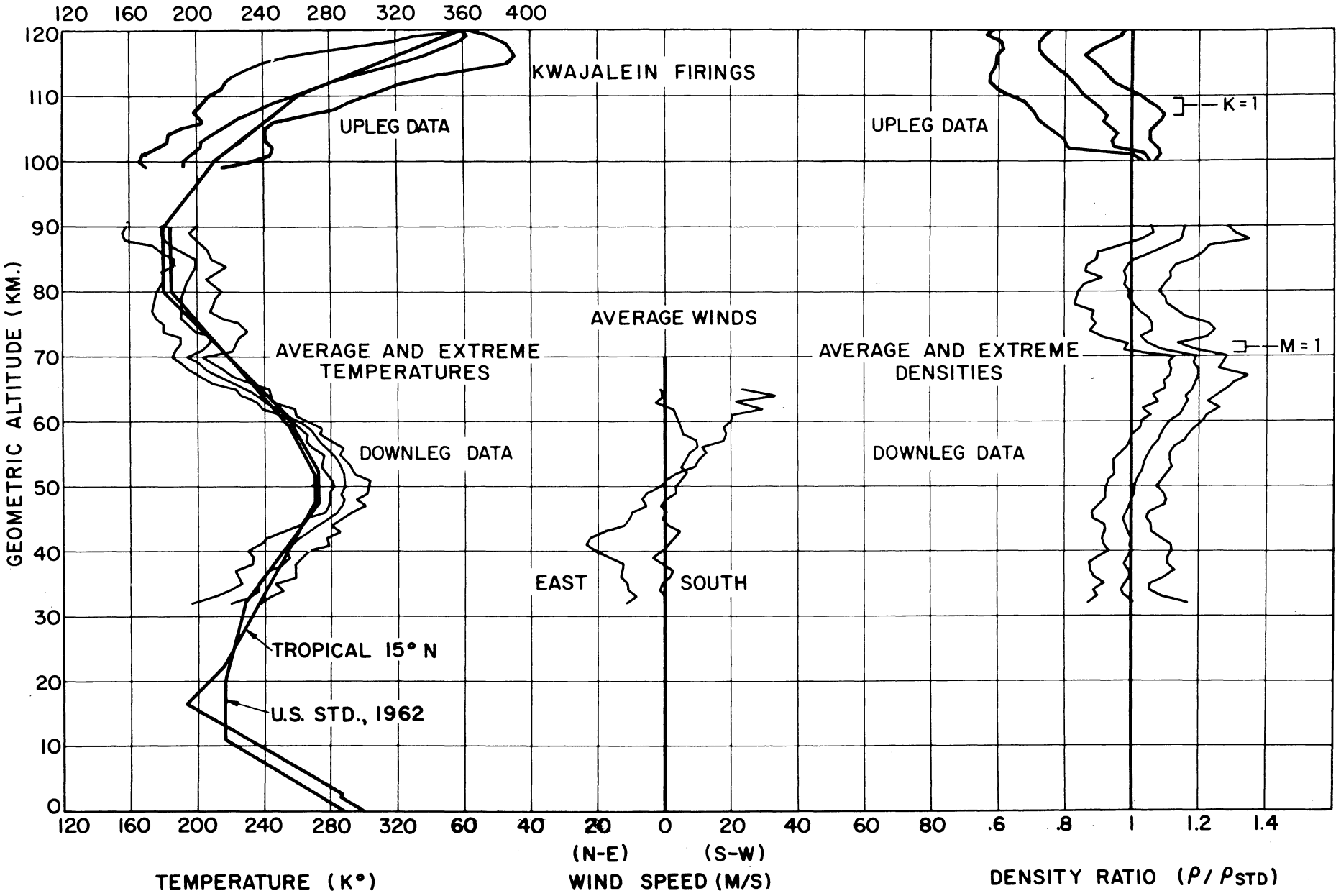

Fig. 11. Average and extreme densities and temperatures and average winds from 13 soundings during all seasons. Kwajalein atoll, 9° 24' N, 1963-64.

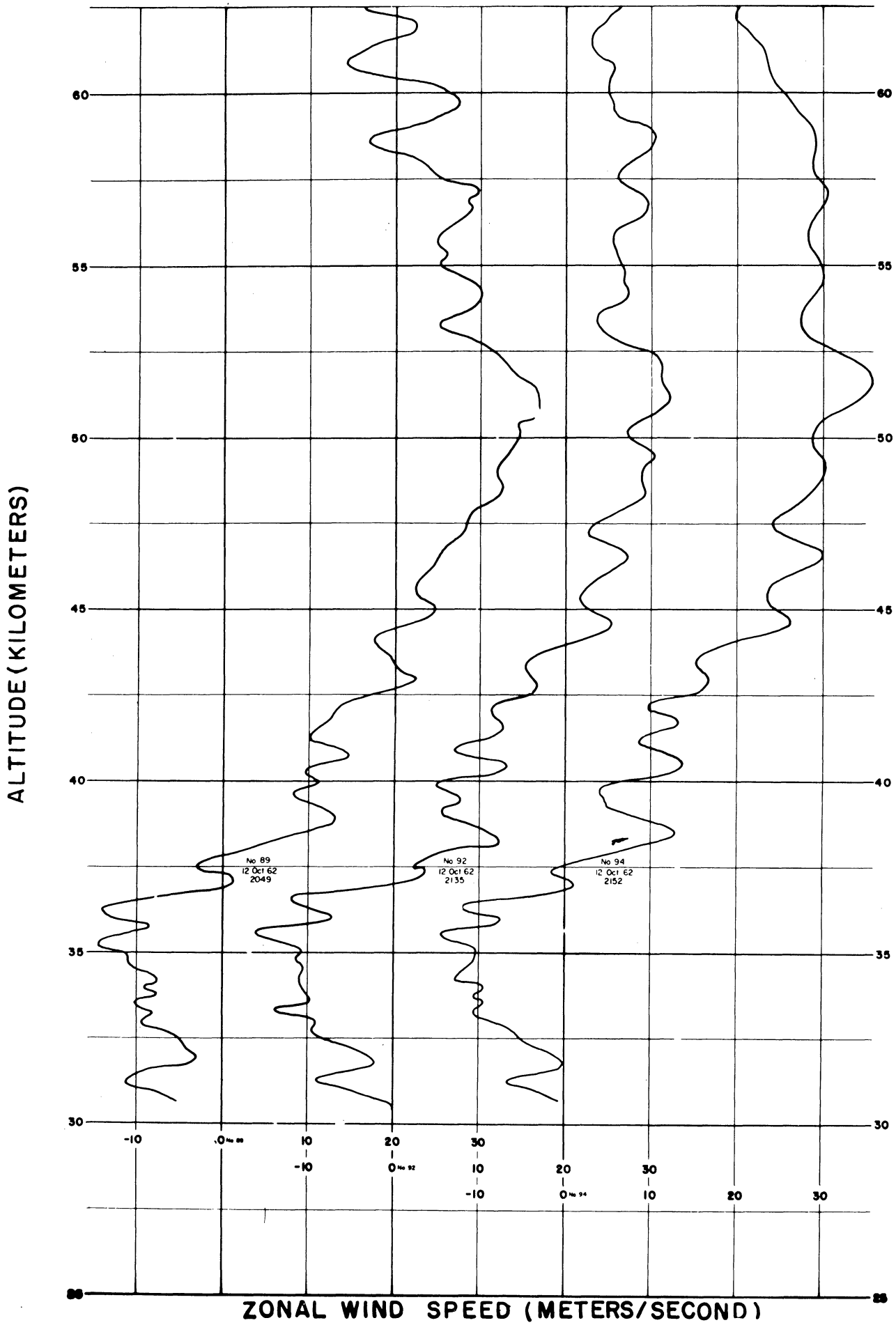

Fig. 12. Zonal wind speed vs altitude. Three sphere soundings at Eglin AFB, 30° 23' N, 1961. After Webb.

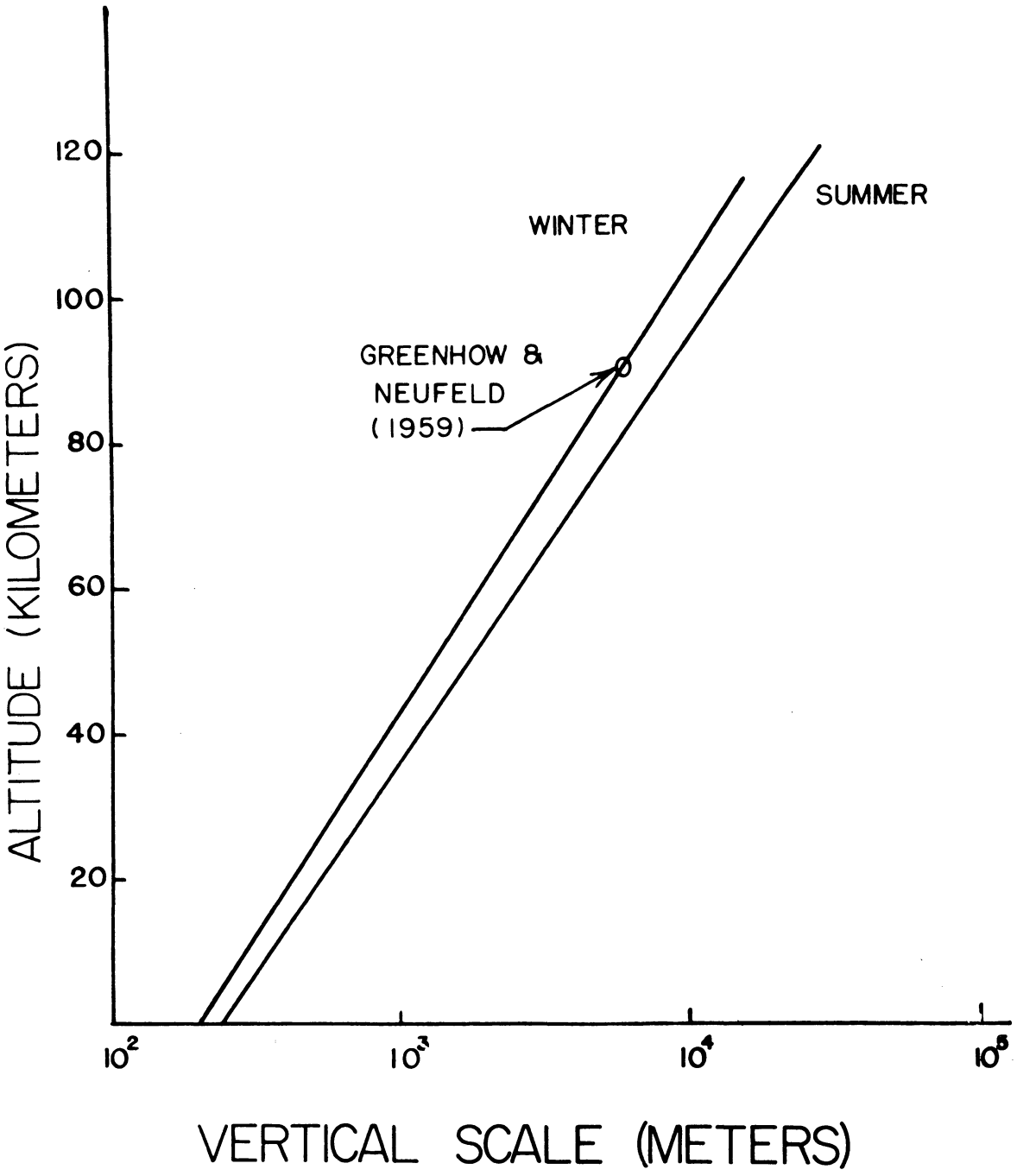

Fig. 13. Vertical scale of wave shapes in wind profiles at Eglin compared with meteor trail echo data. After Webb.

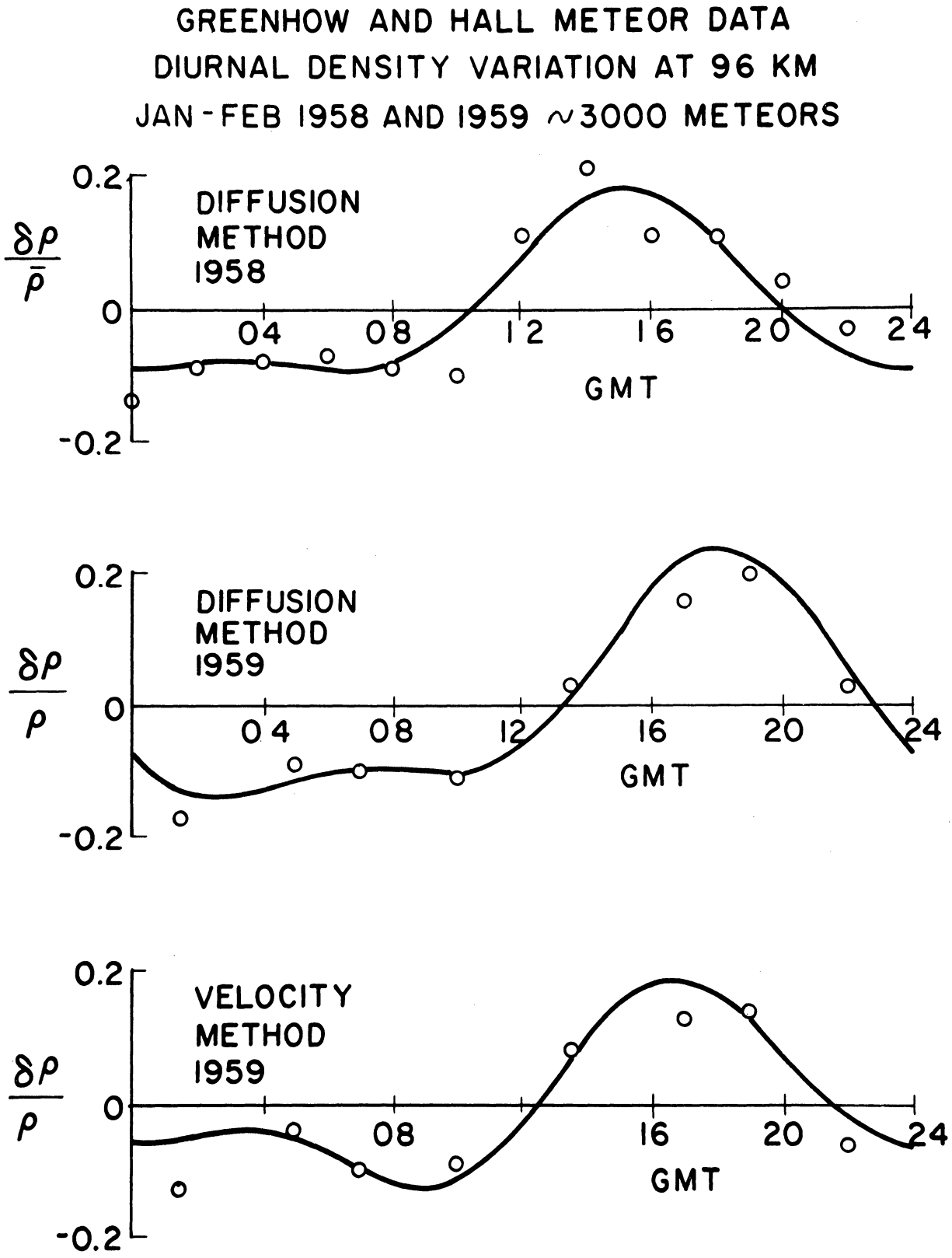

Fig. 14. Diurnal density variations at 96 km from meteor data. After Greenhow and Hall.

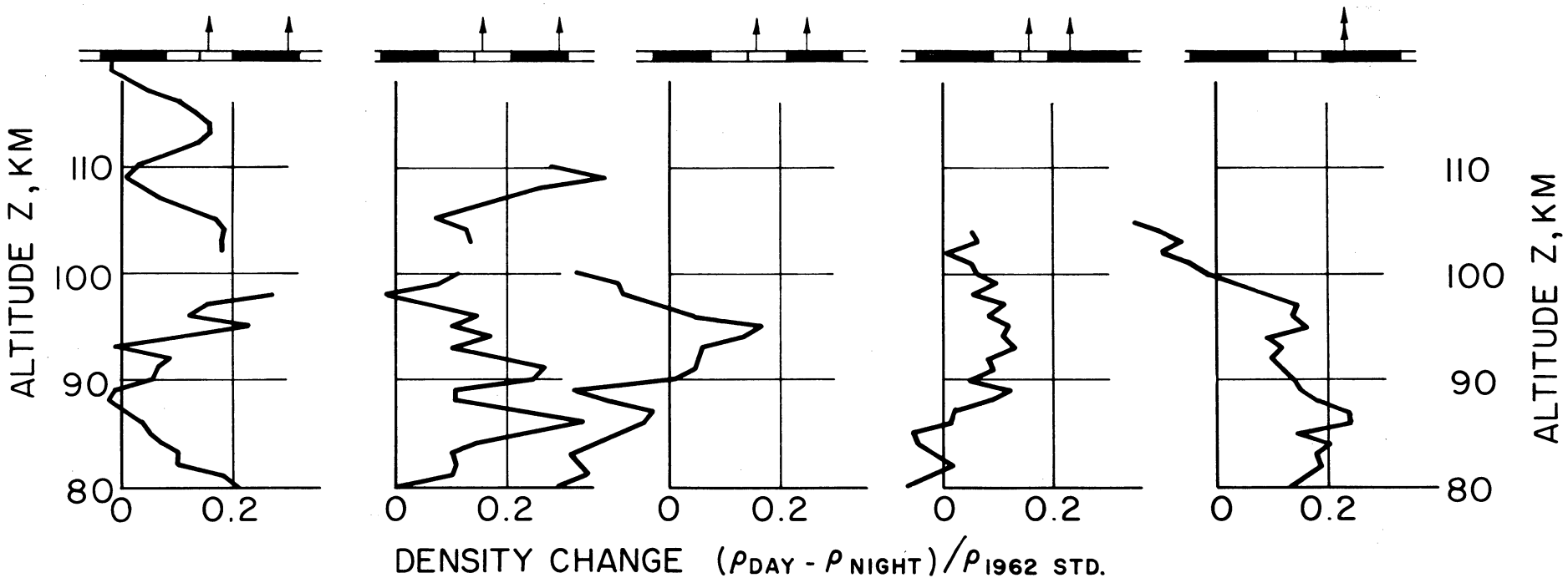

Fig. 15. Diurnal density variations from falling sphere soundings. Peterson and McWatters.

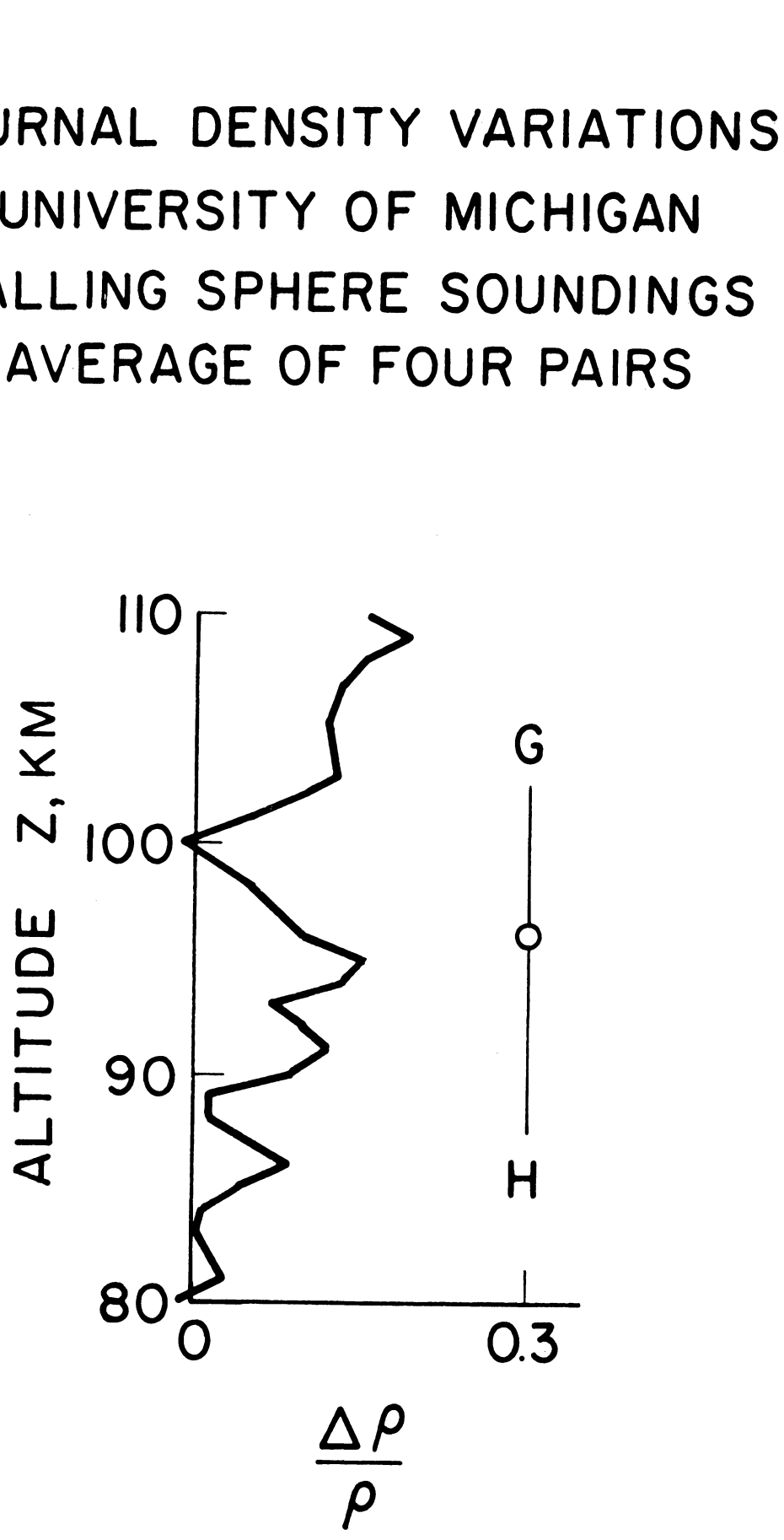

Fig. 16. Average diurnal density variation from four pairs of sphere soundings compared with a meteor observation. Peterson and McWatters.